

# Development of a ferroelectric cathode diode

LI Ruo-Yun(李若云) ZHENG Shu-Xin(郑曙昕)<sup>1)</sup> TANG Chuan-Xiang(唐传祥)

Department of Engineering Physics, Tsinghua University, Beijing 100084, China

**Abstract** As a promising kind of high current cold cathode, the Ferroelectric Cathode (FEC) has several significant advantages, such as a controllable trigger time, lower vacuum requirement and large emitting area fabricability. The emitting current density of the FEC fabricated at Tsinghua University was more than 200 A/cm<sup>2</sup>. In order to make the ferroelectric cathode into practical applications, a high current density diode using a ferroelectric cathode was designed, based on the PIC simulation. The performance of the FEC diode was investigated experimentally. When the applied diode voltage was 60 kV, a current density of more than 250 A/cm<sup>2</sup> was obtained, and the current density distribution was also measured.

**Key words** FEC, high current density diode, plasma

**PACS** 52.75.Fk, 85.50.-n

## 1 Introduction

The use of ferroelectric materials as electron emitters was proposed by Miller and Savage in 1960 [1]. Electron emission from ferroelectrics during the pyroelectric effect was observed by Rosenblum et al. in 1974 [2]. Rosenman and Pechorskii observed emission from ferroelectrics during the piezoelectricity effect in LiNbO<sub>3</sub> in 1980 [3]. The current density measured in these two cases did not exceed 10<sup>-9</sup>–10<sup>-14</sup> A/cm<sup>2</sup>. Studies of the ferroelectric emission during spontaneous polarization reversal in ferroelectric Pb<sub>5</sub>Ge<sub>3</sub>O<sub>11</sub> allowed the observation of the current several orders of magnitude higher, reaching 10<sup>-7</sup> A/cm<sup>2</sup> [4]. These studies are related to the “weak ferroelectric emission”.

In 1989, “strong ferroelectric emission” with a current density reaching 100 A/cm<sup>2</sup> was obtained by Gundel and Reige through the use of ferroelectric PLZT ceramics [5]. Then, studies of this new generation of electron cathodes were carried out all over the world. Because of their advantages, ferroelectric cathode were used in many kinds of electron guns. The high-current gun with a ferroelectric cathode fabricated at Cornell reached a current of 200 A at a diode voltage of 500 kV [6]. The high-current large-area gun using seven ferroelectric cathodes developed by J. Z. Gleizer et al. generated a uniform electron

beam with a cross-sectional area of about 170 cm<sup>2</sup> [7]. The applications of ferroelectric cathodes for microwave generation were carried out at Cornell in the US and Tel Aviv in Israel [8, 9].

In China, the studies of ferroelectric cathodes are mainly carried out at Tsinghua University, Northwest Institute of Nuclear Technology, the China Academy of Engineering Physics, University of Electronic Science and Technology of China, Xi’an Jiaotong University, Shanghai Institute of Ceramics of Chinese Academy of Sciences and so on. In 2007, a ferroelectric gun was fabricated at Tsinghua University. However, the current density was relatively low [10]. In this paper, a recently designed and fabricated ferroelectric cathode diode is reported. In the experiments of this diode, a current density over 250 A/cm<sup>2</sup> is obtained, and the density distribution of the electron beam is measured.

## 2 Design of the ferroelectric cathode diode

Considering our existing facilities, the most suitable parameters for the diode are selected by simulations using the Particle In Cell (PIC) code. The diode structure used in the simulations and the results are shown in Fig. 1. The emitting surface has a diameter of 11 mm. In order to avoid field emission,

Received 10 October 2009

1) E-mail: zhengsx@tsinghua.edu.cn

©2010 Chinese Physical Society and the Institute of High Energy Physics of the Chinese Academy of Sciences and the Institute of Modern Physics of the Chinese Academy of Sciences and IOP Publishing Ltd

the distance between the anode and the cathode is chosen to be 6 mm. The diameter of the anode hole is 15 mm, and a collector is set 1.5 mm away from the

anode hole. In the simulations, the diode voltage is set to be 80 kV, which is the maximum of our power supply.

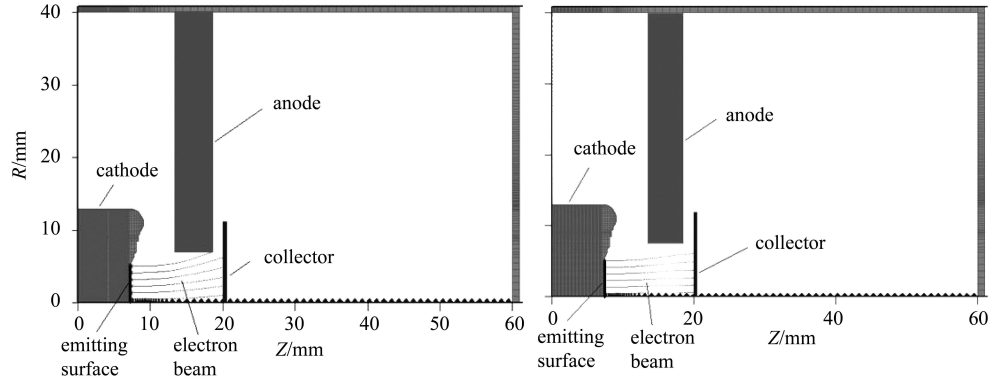


Fig. 1. The diode structure used in the simulations and the results (left: the simulation result without a focusing magnetic field, right: the simulation result with a focusing magnetic field of 0.35 T).

The dashed lines in Fig. 1 represent the electron beam emitted by the ferroelectric cathode. By comparing the two figures in Fig. 1, the necessity of a focusing magnetic field is revealed. It is obvious that part of the electron beam would be captured by the anode without the focusing magnetic field. However, if a focusing magnetic field of 0.35 T were applied in the simulating area, the whole electron beam would be captured by the collector without hitting the anode. A current density of about  $100 \text{ A/cm}^2$  was obtained in the simulation.

Based on the data obtained in the simulations, a ferroelectric cathode diode was fabricated and a focusing magnetic field was applied to make sure that the whole electron beam could go through the anode hole. The ferroelectric cathode was based on a  $\text{Ba}_{0.65}\text{Sr}_{0.35}\text{TiO}_3$  ceramic of 2.3 mm in thickness. The emitting surface was 11 mm in diameter. The front electrode was in the form of copper strips that were glued to the front surface. We used strips of 0.7 mm in width and 0.4 mm in spacing. The rear copper disk electrode was glued to the back surface. The thickness of both the front electrode and the rear electrode was 0.08 mm.

### 3 Experimental setup

The experimental setup mainly consisted of five systems: the high voltage pulse generating system, the driving pulse generating system, the ferroelectric diode system, the diagnostic system and the vacuum system.

#### 3.1 High voltage pulse generating system

The high voltage pulse generating system is shown schematically in Fig. 2. A Marx-Blumlein high voltage pulse generator was used to produce a 60 kV, 80 ns output voltage pulse to the diode in our experiment. This system was controlled by a timer to make sure that the high voltage pulse was generated when the focusing magnetic field was at its maximum (which will be discussed later). The output impedance of the high voltage pulse generator was  $12.5 \Omega$ , but the impedance of the transmission line was  $62.5 \Omega$ . As a result, a  $15.6 \Omega$  water resistor was connected in parallel with the transmission line to match the  $12.5 \Omega$  impedance of the high voltage pulse generator. Since the impedance of the ferroelectric diode was much

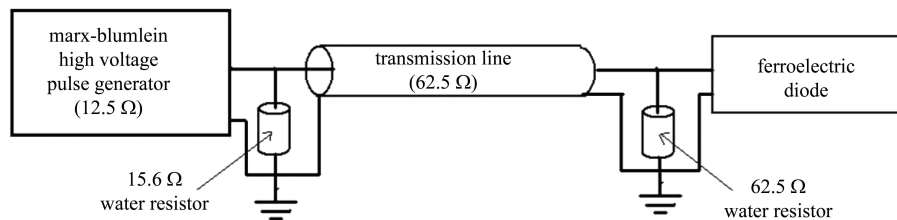


Fig. 2. The high voltage pulse generating system.

higher than the impedance of the transmission line, a  $62.5\ \Omega$  water resistor was connected in parallel with the diode to match the impedance of the  $62.5\ \Omega$  transmission line.

### 3.2 Driving pulse generating system

As shown in Fig. 3, the driving pulse generating system consists of four pulse generators and a 1:1 transformer. Each pulse generator produces a 0–1 kV, 200 ns output voltage pulse. The output voltage on the secondary winding is the sum of all the voltages appearing on the primary windings. As a result, the output pulse voltage is adjustable in a range from 0 to 4 kV. The transformer also keeps the pulse generators insulated from the 60 kV, 80 ns pulse. Under the control of the four timers, the four pulse generators work synchronously. The rise time of the output pulse can be limited to less than 40 ns, and the duration of the output pulse is set to 200 ns. The output pulse is applied to the ferroelectric cathode as a driving pulse. The potential of the front electrode is higher than that of the rear electrode.

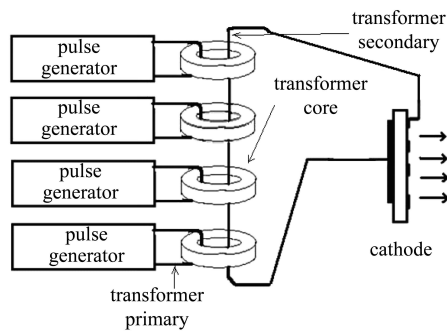


Fig. 3. The driving pulse generating system.

### 3.3 Ferroelectric diode system

As shown in Fig. 4, the ferroelectric diode system consists of the ferroelectric diode and the focusing magnetic field system. The structure of the ferroelectric diode is based on the simulation results discussed in the previous section. The emitting surface is 11 mm in diameter, and the distance between the cathode and the anode is 6 mm. The anode hole is 15 mm in diameter, and a collector is set 1.5 mm away from the anode hole.

A focusing solenoid is used to supply the focusing magnetic field. To achieve the required magnetic field of 0.35 T, the current in the coil should be more than 100 A. In order to reduce the heat generated by the solenoid, three capacitors are used to produce the current pulse in the solenoid. The current in the

coil changes with time because of the C-L oscillation. A timer is used to make sure that the high voltage pulse applied to the cathode is triggered 70 ms after the capacitors begin to charge the focusing solenoid, when the current in the focusing solenoid is at its peak value. As a result, the electron beam is focused by the strongest magnetic field, which is approximately 0.35 T.

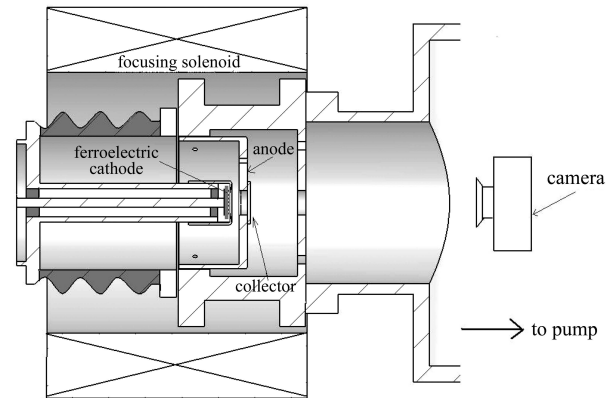


Fig. 4. Structure of the ferroelectric diode system.

### 3.4 Diagnostic system

Since the electron beam was well focused by the magnetic field, it would go through the anode hole and be captured by the collector. Two different kinds of collectors were used in two different experiments. To measure the current density, we used a piece of copper plate as the collector, which was insulated from the anode and connected to the ground by a wire. The current in the wire was equal to the current emitted by the ferroelectric cathode; thus a PEARSON CURRENT MONITOR (MODEL 6595) was used to measure the current in the wire. To measure the density distribution of the current, a YAG screen was used as the collector. When the YAG screen is hit by the electron beam, light was generated and the density distribution of the light would represent the density distribution of the current. As shown in Fig. 4, a camera was set to take the photograph of the light density distribution on the YAG screen and further analysis would show the density distribution of the current.

### 3.5 Vacuum system

The experiment was performed in a vacuum of  $10^{-4}$  Pa, which was maintained by a two-stage pumping system. The first stage is the mechanical pump and the second stage is the turbo-molecular pump.

## 4 Experimental results

### 4.1 Current density measurement

The plasma generated by the driving pulse, which was applied to the front and rear electrodes of the ferroelectric ceramic, played a significant role in the “strong ferroelectric emission” [11]. The mechanism of electron emission from  $\text{Ba}_x\text{Sr}_{(1-x)}\text{TiO}_3$  ceramics has been ascertained for surface plasma emission by Shu-tao Chen [12]. The microgaps between the front electrode and the ferroelectric ceramic surface significantly enhance the electric field by  $E \approx \varepsilon U_0/\delta$ . This makes the electric field as high as  $10^6\text{--}10^7$  V/cm, which causes field emission [13]. The tangential component of the electric field causes electron avalanching along the surface of the ceramic, and the surface plasma is formed [14]. The plasma expands not only along the surface of the cathode but also inside the gap between the anode and the cathode [11]. This enlarges the emission area and reduces the distance between the anode and the cathode. If the diode voltage is applied at the proper time, when the plasma has well covered the surface of the cathode and shortened the distance between the anode and the cathode, a current much greater than the “space-charge-limited current” is gained. In our experiment, the 1.2 kV, 200 ns driving pulse was applied to the electrodes on the surface of the ferroelectric cathode. After a certain delay time, which gives the plasma sufficient

time to cover the surface of the cathode and shorten the distance between the anode and the cathode, the high voltage pulse was applied to the diode. The current waveform shown in Fig. 5 was obtained when the delay was 1  $\mu\text{s}$ . The peak value of the current was 256 A and the emission area of the cathode was  $0.95\text{ cm}^2$ . The current density was  $269\text{ A/cm}^2$ . The current density obtained in the experiment was much larger than that obtained in the simulation, because the distance between the anode and the cathode was reduced by the plasma.

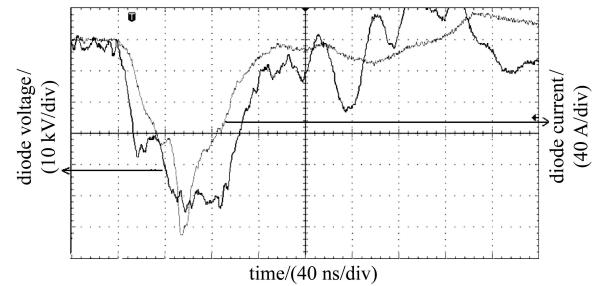


Fig. 5. Waveform of the diode voltage and the current when the delay time was 1  $\mu\text{s}$ .

### 4.2 Observation of the current density distribution

In this experiment, a YAG screen and a camera were used to observe the distribution of the current density. The light density distribution on the YAG screen would well represent the density distribution

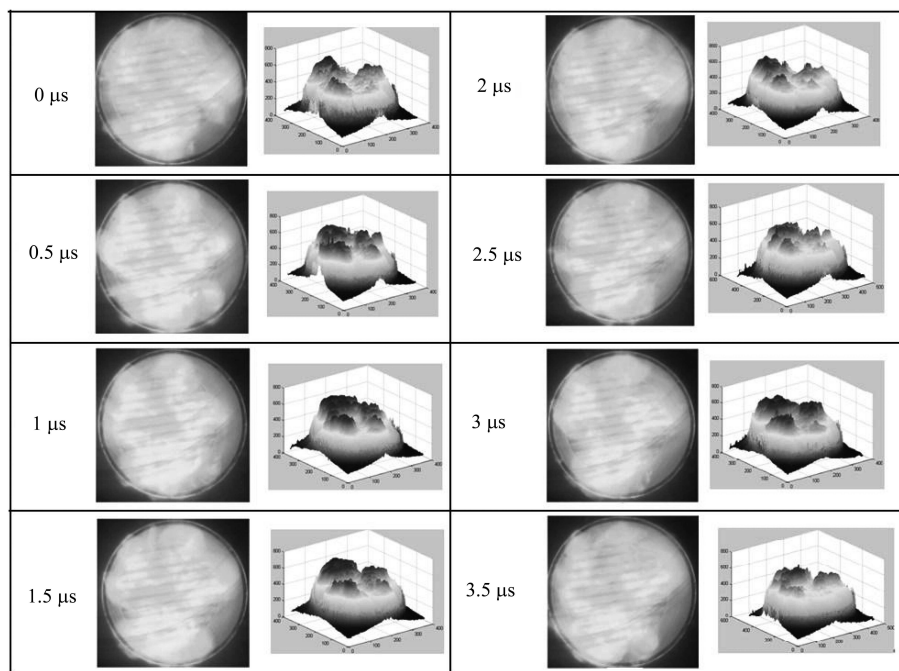


Fig. 6. Photographs of the light on the YAG screen and the current density distribution with different delay times.

of the current. The camera was used to record the light emitted by the YAG screen. As shown in Fig. 6, the current density distribution with different delay times between the driving pulse and the high voltage pulse applied to the diode was recorded. By further analysis with the maths program, the density distribution varying with the delay time could be demonstrated more clearly. Further study is needed to explain the relation between the current density distribution and the delay time, which would benefit the study of the emission process of the ferroelectric cathode.

## 5 Conclusion

By controlling the time delay between the driving pulse and the high voltage pulse applied to the diode, we have obtained a current density of  $269 \text{ A/cm}^2$ , which is much larger than the “space-charge-limited current”. The current density distribution is observed under different delay times. These two experiments are just the beginning. Further study of the relation between the delay time and the current density and its distribution should be carried out.

---

## References

- 1 Miller R, Savage A. *J. Appl. Phys.*, 1960, **31**: 662
- 2 Rosenblum B, Braunlich P, Carrico J P. *Appl. Phys. Lett.*, 1974, **25**: 17
- 3 Rosenman G, Pechorskii V. *J. Exp. Theor. Phys.*, 1980, **6**: 661
- 4 Rosenman G, Okhapkin V, Chepelev Yu, Shur V. *J. Exp. Theor. Phys.*, 1984, **39**: 477
- 5 Gundel H, Reige H. *Nucl. Instrum. Methods Phys. Res. A.*, 1989, **280**: 1
- 6 Yasushi Hayashi, Donald Flechtner, Czeslaw Golkowski et al. *Jpn. J. Appl. Phys.*, 2001, **40**: 397
- 7 Gleizer J Z, Yarmolich D, Vekselman V et al. *Plasma Devices and Operations*, 2006, **14**(3): 223
- 8 Yasushi Hayashi, SONG X, Ivers J D, Donald D. Flechtner, J, A. Nation Levi Schachter. *IEEE Trans. Plasma Sci.*, 2001, **29**(4): 599
- 9 Einat M, Jerby E, Rosenman G. *J. Appl. Phys.*, 2003, **93**(4): 2304
- 10 ZHU Zi-Qiu, ZHENG Shu-Xin, LIAO Shu-Qing, CHENG Cheng, XING Qing-Zi, LI Quan-Feng. *High Power Laser and Particle Beams*, 2008, **20**(3): 521 (in Chinese)
- 11 Shur D, Rosenman G, Krasik Ya E, Kugel V D. *J. Appl. Phys.*, 1996, **79**(7): 3669
- 12 CHEN Shu-Tao, DONG Xian-Lin, ZHENG Shu-Xin et al. *Journal of the American Ceramic Society*, 2006, **89**(7): 2118
- 13 Puchkarev V F, Mesyats G A. *J. Appl. Phys.*, 1995, **78**(9): 5633
- 14 Krasik Ya E, Dunaevsky A, Felsteiner J. *J. Appl. Phys.*, 1999, **85**(11): 7946